Fabrication and Characterization of Polymer-Bonded Flexible Anisotropic Micro-Magnet Arrays

Erika Fontana, Lucie Motyckova, Caterina Tomba, Frederico Orlandini Keller, Georgiana Groza, Marlio Bonfim, Laurent Ranno, Thibaut Devillers, Nora Dempsey

Fabrication and characterisation of polymer-bonded flexible anisotropic micro-magnet arrays

Erika Fontana[1], Lucie Motyckova[1], Caterina Tomba[2], Frederico Orlandi Keller[1], Georgiana Groza[1], Marlio Bonfim[3], Laurent Ranno[1], Thibaut Devillers[1] and Nora M. Dempsey[1]

[1]Université Grenoble Alpes, CNRS, Grenoble INP, Institut Néel, 38000 Grenoble, France
[2] Univ Lyon, CNRS, INSA Lyon, ECL, UCBL, CPE Lyon, INL, UMR5270, 69622 Villeurbanne, France
[3]Universidade Federal do Paraná, DELT, Curitiba, 81531-980, Brazil

Here we present a process for the fabrication of arrays of anisotropic flexible bonded micro-magnets attached to a transparent base. The micro-magnets are based on hard magnetic SmFeN or Sr-ferrite powders mixed with polydimethylsiloxane (PDMS). The size, shape and distribution of the micro-magnets are defined using a Si-mould fabricated by deep reactive ion etching (DRIE). The volume fraction of the magnetic powder was fixed at 30% while the thickness of the micro-magnets ranged from 50-300 µm and their in-plane dimensions from 20-400 µm. Powder alignment was achieved using a bulk NdFeB magnet. Arrays of micro-pillars of height 300 µm and width tapering from 300 µm at their base to 200 µm at their top were characterized using vibrating sample magnetometry (VSM) and Scanning Hall Probe Microscopy (SHPM) and the results of the latter were compared with analytical simulations. The homogeneous magnetic field produced by a 3-axis electromagnet was used to move the micro-pillars in a controlled fashion. The field induced in-plane displacement of the SmFeN-based pillars was more than three times greater than that of the Sr-ferrite-based ones, reaching 13 µm at the maximum applied field value of 100 mT.

***Index Terms*— anisotropic bonded magnet, flexible polymer-bonded magnet, hard magnetic material, SmFeN.**

I. Introduction

Permanent magnets are widely used in many applications, such as motors, audio equipment, actuators and sensors. Depending on the application needs, bulk magnets may be sintered, or polymer bonded. The highest remanence values are achieved in anisotropic fully dense sintered magnets. The remanence of bonded magnets is necessarily limited by the dilution of the magnetic material in a non-magnetic matrix, while higher values are achieved in anisotropic bonded magnets compared to isotropic ones. Nevertheless, bonded magnets are widely used for the following reasons: firstly, they are cheaper than sintered versions in both material and fabrication cost, secondly, they can be easily manufactured in complex geometries, and finally, the mechanical properties can be tuned according to the choice of matrix. Traditional fabrication routes for polymer bonded magnets include calendering, injection moulding, extrusion, and compression bonding [1] while more recently 3D printing of polymer bonded magnets has been explored, in some cases down to the mm size range [2]–[7]. Down-scaling the size of magnets opens new opportunities for their use in micro-devices with applications in fields as diverse as telecommunications, energy management and bio-medicine. Sputtering combined with micro-patterning has been used to make fully dense magnets which are a micro-scale equivalent of sintered magnets and they may be isotropic or textured, depending on the deposition temperature [8]–[10]. Various techniques including casting and screen printing combined with photo-lithography have been used to make polymer bonded micro-magnets, but micro-scaled polymer bonded magnets reported to date are isotropic [10]–[13]

In this article we present a process for the fabrication of anisotropic flexible bonded micro-magnets. Anisotropic powders were selected to maximise the magnetisation for a given volume fraction of magnetic material and to favour actuation through the use of magnetic torque [14], [15]. Micro-magnets were prepared using commercial single crystalline hard ferrite Sr-ferrite ($SrFe_{12}O_{19}$) and SmFeN ($Sm_2Fe_{17}N_x$) mixed with polydimethylsiloxane (PDMS). Note that commercial NdFeB powders of comparable size are nanocrystalline and isotropic, and thus cannot be used to make anisotropic bonded micro-magnets. PDMS was chosen as the binder so as to have flexible micro-magnets that could potentially be used in bio-medical applications. We present results of both magnetic characterisation of the micro-magnets and preliminary actuation tests [16].

FIG. 1 HERE

II. Experimental procedures

The process we developed for the fabrication of arrays of anisotropic bonded magnets is schematised in Fig. 1. The basic idea is to use a Si-mould to define the size, shape and distribution of individual micro-magnets, and then to transfer the array of micro-magnets to a PDMS base layer. Having a transparent base layer will facilitate the use of the micro-

Manuscript received April 1, 2015; revised May 15, 2015 and June 1, 2015; accepted July 1, 2015. Date of publication July 10, 2015; date of current version July 31, 2015. (Dates will be inserted by IEEE; "published" is the date the accepted preprint is posted on IEEE Xplore®; "current version" is the date the typeset version is posted on Xplore®). Corresponding author: F. A. Author (e-mail: f.author@nist.gov). If some authors contributed equally, write here, "F. A. Author and S. B. Author contributed equally." IEEE Transactions on Magnetics discourages courtesy authorship; please use the Acknowledgment section to thank your colleagues for routine contributions.

Color versions of one or more of the figures in this paper are available online at http://ieeexplore.ieee.org.

Digital Object Identifier (inserted by IEEE).

magnets in bio-applications, where imaging is most typically done in transmission mode. Moreover, PDMS is chemically inert, permeable to gases and thermally stable, and therefore widely used for microfluidic and micro-devices for biological applications.

Patterned Si-moulds were prepared by a microfabrication process involving photolithography through a mask followed by deep reactive ions etching (DRIE). 4-inch Si-wafers (525 μm thick) were first coated with 6 μm of positive resist (AZ4562) and then baked at 100° C for 90 s. The coated wafers were exposed through a mask using UV light for 30 s at a constant dose of 150 mJ/cm2, then the non-exposed resist was removed by development in a solution of AZ-developer for 30 s. We etched features in the Si-substrate by DRIE, a process based on the repetition of two modes: plasma etching (SF_6) to attack the Si-substrate and deposition of a passivation layer (C_4F_8) to avoid side etching. We varied the ratio of the duration of the modes to modify the depth (max 300 μm) and the angle (67-90°) of the etched features.

We prepared the PDMS binder by mixing the elastomer base and curing agent in a ratio of 1:10 and then degassed it in a desiccator under primary vacuum for 1-2 h, to remove the air bubbles formed by stirring the two components. The magnetic composite was prepared by mixing the PDMS with the magnetic powder. SEM images of the commercial Sr-ferrite (Dowa OP-71) and SmFeN (Nichia Z12) single crystalline powders used here are shown in Fig. 2. The average particle size is 1.5 μm and 3 μm for the Sr-ferrite and SmFeN particles, respectively, with the former showing a wide distribution in particle size. The ferrite powder has more moderate magnetic properties (Br: ~ 400 mT, Hc: 123 kA/m) than the SmFeN powder (Br: 1.31 T, Hc: 889 kA/m). The powder concentration in the mixture was set at 30 volume % and the magnetic mixture was degassed for 5-10 minutes in a desiccator under vacuum to remove bubbles.

FIG. 2 HERE

We diced the Si-mould into mm-sized chips, then using a spatula we spread the magnetic mixture into the mould cavities and we removed the excess material using the doctor blade technique. We tested two different types of magnetic field source to achieve powder alignment: (1) a bulk magnet (NdFeB of size 2.4×2.4×4.8 cm^3, producing a stray field of intensity 650 mT at its surface); (2) pulsed-field systems producing μs and ms pulses of maximum field intensity 10 T and 2.5T, respectively). To prevent particles moving out of the mould during alignment, a thin lamina of glass (about 0.1 mm thick) was used to cover the filled mould, and the covered samples were baked in an oven at 70°C. The duration of this soft curing step was varied from 30 minutes to 1 hour. Following the removal of the glass coverslip, a layer of PDMS was poured on the sample before making the final bake. After 3h at 70°C in the oven the samples were completely cured, and they could easily be peeled off the Si mould.

A Vibrating Sample Magnetometer (VSM) with a maximum field of 8T was used to measure the degree of alignment of the powders, by comparing magnetisation measurements made with the applied field parallel and perpendicular to the direction of alignment. Isotropic micro-magnet arrays, prepared without an applied magnetic field, were used as reference samples. As the flexible micro-magnets can be deflected upon application of a magnetic field, magnetisation measurements were made just after the hard curing, when the structures were still in the Si mould. Additional measurements were made on fully processed samples, which were "frozen" by impregnation in epoxy resin.

The out-of-field (B_z) component of the stray field produced by the micro-magnets was quantified using a Scanning Hall Probe Microscope (SHPM) [17]. This system has a field resolution of 100 μT and can scan areas up to a few mm in-plane (0.1 μm step resolution). We made analytical simulations of the stray field generated by the microstructures using the method described in [18]. The expected magnetic field profile was calculated based on the micro-magnet geometry and the magnetization and volume fraction of the magnetic powder. The simulation is valid just for rectangular parallelepiped magnets, but two parallelepipeds can be considered to approximate the tapered down shape of the structures.

Actuation tests were performed using a 3-axis electromagnet mounted on an optical microscope. The field source allows the application of a homogeneous magnetic field with control over all three spatial components, and the maximum field intensity for the pole gap used here was roughly 100 mT. Distortion of the micro-magnets under the influence of an applied field was captured by sequential imaging, and displacement of the top of the micro-magnets was quantified by computing autocorrelations between images.

I. Results and discussion

Micro-magnets were fabricated with different geometries (squares and stripes) of width in the range 20 to 400 μm (the length of the stripes was set at 4 mm) and thickness in the range 50 - 300 μm. Visual inspection of fully cured structures with mixed feature geometry and width (such as the sample shown in Fig. 1) indicated that a shorter soft-curing of 30 minutes is better suited to structures of width < 100 μm, meaning the powder appears homogeneously distributed in the binder, while the longer time of 60 minutes is better suited to larger structures. The results presented hereafter concern arrays of micro-pillars made using a Si mould prepared with a mask of square features with in-plane dimensions 300x300 $μm^2$. The Si was etched 300 μm in depth, and the width of the etched holes tapered down from 300 μm at the surface of the mould to roughly 200 μm at the base of the etch. A cross-section image of a micro-magnet is shown in Fig 4.

FIG. 3 HERE

Hysteresis loops measured on non-aligned reference samples and samples aligned using the bulk magnet are compared in Fig 3. The direction of the external applied field

FIG. 4 HERE

FIG. 5 HERE

is indicated with respect to the plane of the 2D array of micro-magnets, i.e. "in plane" is perpendicular to the direction of alignment defined in Fig. 1, while "out-of-plane" is parallel to it. As expected, there is no difference in the shape of the curves of the reference isotropic sample. The aligned samples show anisotropic behaviour, with the out-of-plane loops having a noticeably higher m_0/m_{max} (magnetisation in zero applied field divided by magnetisation in maximum applied field) than the in-plane loops 3 times higher for the ferrite-based sample and 2 times higher for the SmFeN-based one. Nevertheless, the non-negligible m_0/m_{max} values measured in-plane suggest that the degree of alignment could be further increased. Hysteresis loops measured with the pillars still in the Si mould are comparable with those measured on pillars fixed in epoxy resin (data not shown). Samples exposed to μs pulsed magnetic fields of intensity 4T were isotropic, as the time scale over which the magnetic torque was applied was insufficient to overcome the viscosity of the binder. On the other hand, those exposed to ms pulses of intensity 2T showed curves comparable to those aligned with the bulk magnet (data not shown). The application of repeat ms pulses did not increase the degree of alignment. Results reported hereafter are for micro-magnets aligned with the bulk magnet.

A 2D map of the z-component of the stray magnetic field measured at an estimated scan height of 50 μm above the SmFeN micro-magnet array is shown in Fig. 4a. Assuming that the density of particles and degree of alignment is equivalent in all micro-magnets, the observed variations in field intensity from the different micro-magnets may be attributed to the tilt of the pillar plane with respect to scanning plane. The plane of measurement is defined by triangulation of three points of contact, and the flexible nature of the micro-magnets complicates the calibration procedure. Nevertheless, such measurements serve to roughly quantify the stray field pattern produced by the micro-magnet array. 1D-scans taken along the dotted line shown in Fig. 4a, measured at estimated heights of 50 μm, 100 μm and 150 μm, are plotted in Fig. 4b and can be compared with analytical simulations shown in Fig. 4c. An optical image of the cross section of a micro-magnet is shown as an inset of Fig. 4b while a schematic of the over-simplified shape of the magnet assumed for the calculations, which consists of two rectangular parallelepiped magnets, is shown as an inset of Fig. 4c. The peak-to-peak intensities of the measured and calculated out-of-plane field components are comparable, being of the order of 100-150 mT at 50 μm, 60-80 mT at 100 μm and 30-50 mT at 150 μm.

A homogeneous magnetic field produced by the 3-axis electromagnet was then used to induce motion of anisotropic Sr-ferrite and SmFeN micro-pillars with base dimensions of 300 × 300 μm^2, 200 × 200 μm^2 top base dimensions and a height of 300 μm^3. The measured in-plane displacements of the top of a micro-pillar from each array, with the actuation field applied perpendicular (x and y directions) and parallel to the direction of the alignment (z direction), are shown in Fig. 5. Note that no displacements of the PDMS base were observed. The in-plane micro-pillar displacement increases linearly with applied field strength when the field is applied in-plane, i.e. perpendicular to the axis of alignment, whereas no out-of-plane displacement is detected when a field is applied parallel to the alignment axis. Both observations are consistent with torque-mode actuation in a homogeneous magnetic field. The slight in plane movement with out of plane applied field is attributed to a small tilt between magnetization and field direction, while the step like behaviour visible in displacement in Z field is due to the function used for the autocorrelation that gives as output integer number of pixels. The Sr-ferrite-based pillar moves 0.04 μm/mT (Fig. 5a) whereas the SmFeN-based pillar moves 0.13 μm/mT (Fig. 5b). The ratio of the displacement (0.13/0.04) matches with the ratio of the remanence magnetization of the constituent magnetic powders (1.3 / 0.4).

II. Conclusion

In this article we presented a relatively simple process for the fabrication of anisotropic flexible bonded micro-magnets based on single crystalline Sr-ferrite or SmFeN hard magnetic micro-sized powders. The micro-magnets ranged in thickness from 50 μm to 300 μm, and width 20 μm to 400 μm and the volume fraction of powder was set at 30%. Similar degrees of powder alignment were achieved using a bulk magnet producing a stray field of 650 mT and a ms pulsed field of maximum intensity 2 T. The stray magnetic field profile produced by an array of SmFeN micro-pillars of base width 300 μm and height 300 μm was measured using a micro-Hall probe scanned at heights of 50, 100 and 150 μm above the array, and reasonable agreement was achieved with simulated stray field profiles. The homogeneous magnetic field produced by a 3-axis electromagnet was used to move Sr-ferrite and SmFeN-based pillars in a controlled fashion. The field induced in-plane displacement (μm/mT) of the SmFeN-based pillars was more than three times greater than that of the Sr-ferrite-based ones, reaching 13 μm at the maximum applied field value of 100 mT. In a follow-on study we plan to characterise the spatial distribution of the magnetic particles as a function of their volume fraction and the applied magnetic field (both field intensity and the type of field source). We will also try to further improve the degree of texture and will assess its influence, as well as that of the volume fraction of magnetic material, the pillar dimensions and aspect ratio, on the extent of magnetically actuated displacement. We will also characterise the mechanical properties of the structures and model their magnetically induced actuation. Altogether, the

results presented here demonstrate the possibility to magnetically actuate micro-structures. The development of similar microstructures of different size and shape will open their use to a wide panel of applications in bio-devices, and in particular for mechanical stimulation of cells inmechanobiology studies.

III. Acknowledgment

This research has received funding from the French National Research Agency under the project HiPerTherMag (ANR-18-CE05-0019). Substrate patterning was carried out on PTA platform. The authors would like to thank Simon Le-Denmat (Institut Néel) for his redevelopment of the Scanning Hall Probe Microscope and Boris Saje (Kolektor) for kindly providing the magnetic particles.

References

[1] J. Ormerod and S. Constantinides, 'Bonded permanent magnets: Current status and future opportunities (invited)', *J. Appl. Phys.*, vol. 81, pp. 4816–4820, 1997.

[2] K. Sonnleitner *et al.*, '3D printing of polymer-bonded anisotropic magnets in an external magnetic field and by a modified production process', *Appl. Phys. Lett.*, vol. 116, pp. 092403, 2020.

[3] K. Gandha, I. C. Nlebedim, V. Kunc, E. Lara-Curzio, R. Fredette, and M. P. Paranthaman, 'Additive manufacturing of highly dense anisotropic Nd–Fe–B bonded magnets', *Scr. Mater.*, vol. 183, pp. 91–95, 2020.

[4] A. P. Taylor, C. Velez Cuervo, D. P. Arnold, and L. F. Velasquez-Garcia, 'Fully 3D-Printed, Monolithic, Mini Magnetic Actuators for Low-Cost, Compact Systems', *J. Microelectromechanical Syst.*, vol. 28, no. 3, pp. 481–493, 2019.

[5] K. Gandha *et al.*, 'Additive manufacturing of anisotropic hybrid NdFeB-SmFeN nylon composite bonded magnets', *J. Magn. Magn. Mater.*, vol. 467, pp. 8–13, 2018.

[6] C. Huber *et al.*, 'Topology optimized and 3D printed polymer-bonded permanent magnets for a predefined external field', *J. Appl. Phys.*, vol. 122, pp. 053904, 2017.

[7] L. Li *et al.*, 'Big Area Additive Manufacturing of High Performance Bonded NdFeB Magnets', *Sci. Rep.*, vol. 6, pp. 36212, 2016.

[8] N. M. Dempsey, A. Walther, F. May, D. Givord, K. Khlopkov, and O. Gutfleisch, 'High performance hard magnetic NdFeB thick films for integration into micro-electro-mechanical systems', *Appl. Phys. Lett.*, vol. 90, p. 092509, 2007.

[9] A. Walther, C. Marcoux, B. Desloges, R. Grechishkin, D. Givord, and N. M. Dempsey, 'Micro-patterning of NdFeB and SmCo magnet films for integration into micro-electro-mechanical-systems', *J. Magn. Magn. Mater.*, vol. 321, pp. 590–594, 2009.

[10] N. M. Dempsey, 'Hard Magnetic Materials for MEMS Applications', in *Nanoscale Magnetic Materials and Applications*, Eds. Boston, MA: Springer US, 2009, pp. 661–683.

[11] H. J. Cho and C. H. Ahn, 'Microscale resin-bonded permanent magnets for magnetic micro-electro-mechanical systems applications', *J. Appl. Phys.*, vol. 93, pp. 8674–8676, 2003.

[12] T.-S. Yang, N. Wang, and D. P. Arnold, 'Fabrication and characterization of parylene-bonded Nd–Fe–B powder micromagnets', *J. Appl. Phys.*, vol. 109, pp. 07A753, 2011.

[13] K. Tao, G. F. Ding, Z. Q. Yang, Y. Wang, and P. H. Wang, 'Fabrication and Characterization of Bonded NdFeB Microstructures for Microelectromechanical Systems Applications', *Adv. Mater. Res.*, vol. 211–212, pp. 561–564, 2011.

[14] T. Fukushi, S. H. Kim, S. Hashi, and K. Ishiyama, 'Magnetic silicone rubber: Fabrication and analysis with applications', *J. Korean Phys. Soc.*, vol. 63, no. 3, pp. 686–690, Aug. 2013.

[15] T. Fukushi, S. Hoon Kim, S. Hashi, and K. Ishiyama, 'Preliminary validation of Sm–Fe–N magnetic silicone rubber for a flexible magnetic actuator', *Smart Mater. Struct.*, vol. 23, pp. 067001, 2014.

[16] N. M. Dempsey, *Magnetism and Biology*, vol. Handbook of Magnetic Materials. Springer, in press.

[17] G. Shaw, R. B. G. Kramer, N. M. Dempsey, and K. Hasselbach, 'A scanning Hall probe microscope for high resolution, large area, variable height magnetic field imaging', *Rev. Sci. Instrum.*, vol. 87, pp. 113702, 2016.

[18] R. Engel-Herbert and T. Hesjedal, 'Calculation of the magnetic stray field of a uniaxial magnetic domain', *J. Appl. Phys.*, vol. 97, pp. 074504, Apr. 2005.

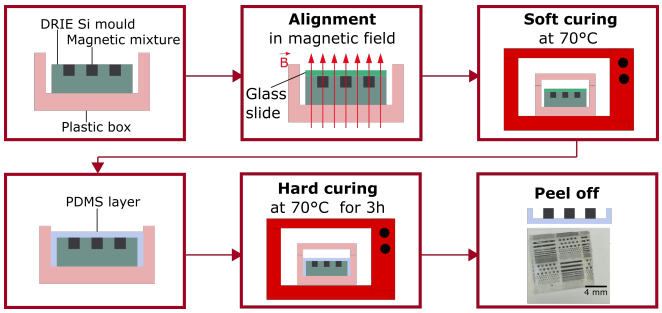

Fig. 1 Schematic of the fabrication process for anisotropic bonded magnets. Single crystalline hard magnetic powders mixed with PDMS are filled into the etched pattern of a Si mould. A magnetic field is used to align the magnetic powders, with a glass slide positioned on top to prevent powder extrusion from the etched features. A soft curing is applied and then a PDMS layer is poured on the structure to form a base for the micro-magnets. The PDMS of the micro-magnets and the base is hard cured and then the structures can be peeled from the Si mould.

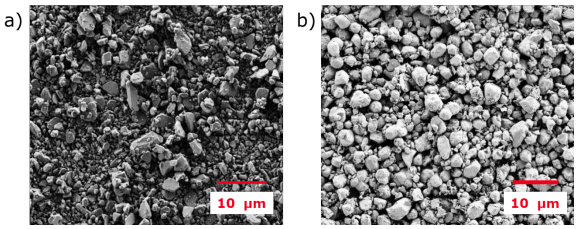

Fig. 2 Scanning Electron Microscope (SEM) images of a) Sr-ferrite powder and b) SmFeN powder.

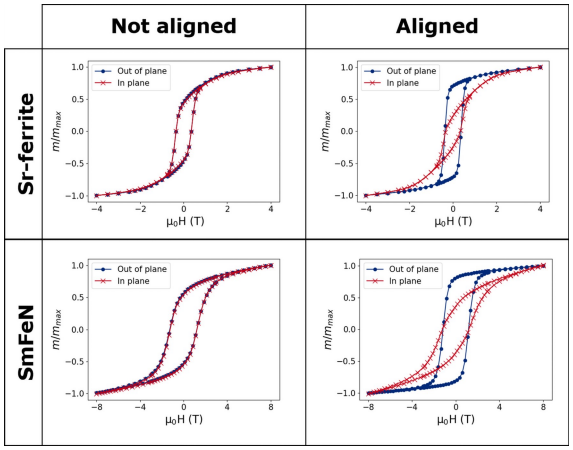

Fig. 3 Normalized magnetic moment vs external magnetic field applied in plane or out of plane with respect to the PDMS base.

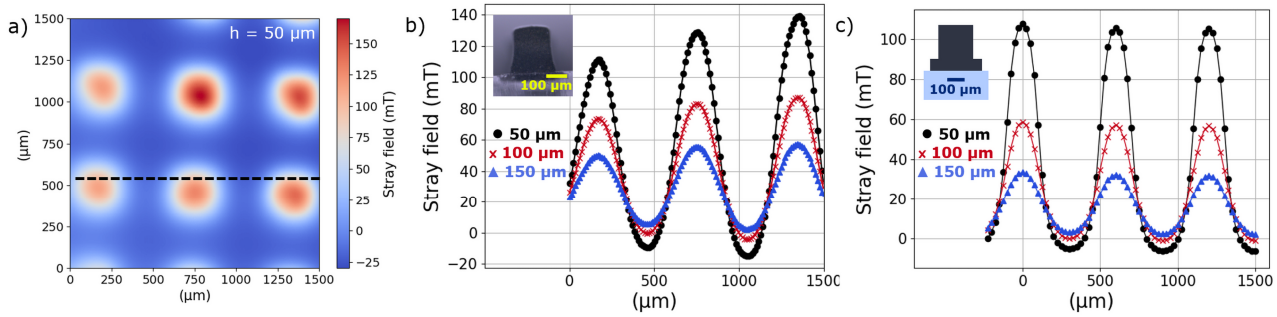

Fig. 4 Measured and calculated stray field pattern produced by the micro-magnet array a) A 2D map of the stray field generated by SmFeN micromagnets at 50 µm from the micromagnet surface, measured by Scanning Hall Probe Microscopy; b) 1D scans made at 50 µm, 100 µm, 150 µm from the micromagnet surface, along the black dotted line indicated in a), and optical image of the cross section of one micromagnet is shown as an inset; c) Analytical calculations performed at 50 µm, 100 µm, 150 µm from the micromagnet surface, a schematic of the simulated structure is shown as an inset.

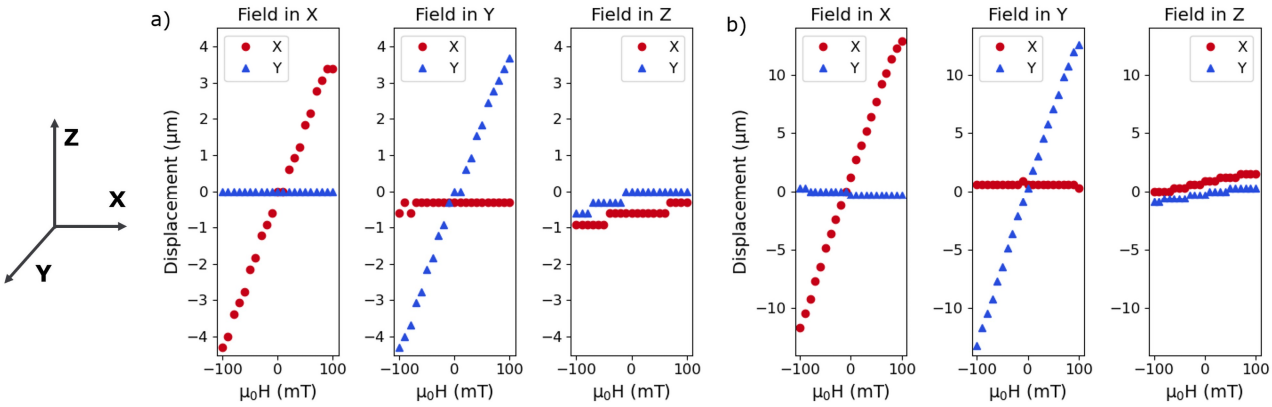

Fig. 5 Displacement of the upper surface of a micro-magnet in the X (red circles) and in Y (blue triangles) directions, for three different orientations of the external applied field: a) Sr-ferrite and b) SmFeN.